

# Superfluidity vs. localization in bulk $^4\text{He}$ at zero temperature

C. Cazorla and J. Boronat

*Departament de Física i Enginyeria Nuclear, Campus Nord B4-B5,  
Universitat Politècnica de Catalunya, E-08034 Barcelona, Spain*

(Dated: October 1, 2017)

We present a zero-temperature quantum Monte Carlo calculation of liquid  $^4\text{He}$  immersed in an array of confining potentials. These external potentials are centered in the lattice sites of a fcc solid geometry and, by modifying their well depth and range, the system evolves from a liquid phase towards a progressively localized system which mimics a solid phase. The superfluid density decreases with increasing order, reaching a value  $\rho_s/\rho = 0.079(16)$  when the Lindemann's ratio of the model equals the experimental value for solid  $^4\text{He}$ .

PACS numbers: 67.80.-s, 02.70.Ss, 67.40.-w

## I. INTRODUCTION

The counterintuitive coexistence of superfluidity and solid order has been the object of theoretical and experimental debate for a long time. The recent experimental findings by Kim and Chan of non-classical rotational inertia (NCRI) in solid  $^4\text{He}$ , both in bulk<sup>1</sup> and in a confined environment,<sup>2,3</sup> suppose a real breakthrough in the field. Using a torsional oscillator setup and ultrahigh-purity  $^4\text{He}$ , a superfluid density  $\rho_s/\rho \sim 1 - 2\%$  has been measured below a temperature  $T = 230\text{mK}$ . The transition temperature from normal solid to supersolid is nearly constant with the pressure and no signal of the transition is observed in the specific heat.<sup>4</sup> On the other hand, other manifestations of superfluidity like pressure-induced flow has not been detected in a recent experiment where solid  $^4\text{He}$  was confined in  $V_{\text{ycor}}$ .<sup>5</sup>

On the theoretical side, the pioneering works by Andreev and Lifshitz<sup>6</sup> and Chester<sup>7</sup> suggested for the first time the possibility of Bose-Einstein condensation of vacancies or interstitials in solid  $^4\text{He}$ . Recently, Prokof'ev and Svistunov<sup>8</sup> have worked out on the same idea and have established that the existence of defects in the solid is a necessary condition for observing superfluidity, i.e., the supersolid phase. According to this mechanism for superfluidity in the solid phase,  $^4\text{He}$  could present at very low temperature the form of an incommensurate crystal, i.e., a quantum solid where the number of lattice sites is different from the number of atoms.<sup>9</sup> Also, the possibility of a disordered solid phase (glass) has been suggested as an alternative for observing superfluid signals.<sup>10</sup> However, the hypothesis of incommensurability contradicts well established experimental data about the absolutely negligible concentration of vacancies at temperatures where supersolid has been observed.<sup>11</sup>

Following Leggett's arguments,<sup>12</sup> a second plausible scenario for a supersolid phase would be the one of a commensurate crystal but with enough exchanges between atoms to generate NCRI. This fascinating possibility can only be thought in a quantum solid such as  $^4\text{He}$  where the displacements of the atoms around the lattice sites are incredibly large from a classical point of view. However, recent path integral Monte Carlo (PIMC) simulations of

solid  $^4\text{He}$  near the experimental transition temperature have not detected neither superfluid density<sup>13</sup> nor off-diagonal long-range order.<sup>14</sup> It is worth mentioning that the estimation of both magnitudes is rather difficult using PIMC since the temperature is very low and the signal is expected to be very small.

Zero-temperature properties of solid  $^4\text{He}$  such as its equation of state, static structure factor or Lindemann's ratio have been calculated using diffusion Monte Carlo (DMC)<sup>15</sup> and Green's function Monte Carlo (GFMC).<sup>16</sup> The results obtained show an excellent agreement with experimental data due to both the exactness of the method and the accuracy of the interatomic potential between helium atoms. However, these calculations use as importance sampling trial wave function a Nosanow-Jastrow (NJ) model,<sup>17</sup> which is not symmetric under the exchange of particles. This is not a drawback for calculations of the energy or the spatial structure since the exchange energy has been estimated to be negligible, about  $3\mu\text{K}/\text{atom}$ ,<sup>13</sup> but the lack of a correct quantum symmetry does not allow for estimations of the one-body density matrix and the superfluid density. Two different models have been proposed to overcome this limitation. The first one is inspired in the Bloch function of band theory currently used for electrons; it is effectively a symmetric trial wave function but has proven to be worse than the NJ model at the variational level.<sup>18</sup> The second one corresponds to the shadow wave function,<sup>19</sup> which allows for a good variational description of the solid, but not yet implemented in a DMC calculation.

In the present work, we present a microscopic study by means of the DMC method of bulk  $^4\text{He}$  immersed in a lattice of confining potentials. By increasing progressively the strength of these external potentials we can get relevant information on the interplay between localization and superfluidity. Measuring the degree of localization through the Lindemann's ratio  $\gamma$  one can compare the physics of this structured phase with the solid one. At the experimental value for  $\gamma$  near the melting point the present model shows a non-zero superfluid fraction, compatible with the existence of a supersolid  $^4\text{He}$  phase at zero temperature.

In the following section, the method used for the calcu-

lation is briefly described. Sec. III comprises the results obtained, and finally, Sec. IV summarizes the work and presents the main conclusions.

## II. METHOD

The  $N$ -body system under study is described by the Hamiltonian

$$H = -\frac{\hbar^2}{2m} \sum_{i=1}^N \nabla_i^2 + \sum_{i<j}^N V(r_{ij}) + \sum_{i,j}^N V_c(|\mathbf{r}_i - \mathbf{R}_j|), \quad (1)$$

with  $V(r)$  the interatomic potential between He atoms, and

$$V_c(r) = -V_0 \exp(-\alpha r^2) \quad (2)$$

are potential wells centered in the positions  $\mathbf{R}_j$ , which correspond to the sites of a solid lattice. The ground-state energy and other relevant properties of the system at zero temperature can be calculated exactly, within statistical errors, using the diffusion Monte Carlo (DMC) method.<sup>20</sup> With DMC, one is able to solve stochastically the  $N$ -body imaginary-time Schrödinger equation by performing a random walk of the walkers ( $\mathbf{R} \equiv \{\mathbf{r}_1, \dots, \mathbf{r}_N\}$ ), which define the wave function, according to a short-time approximation for the Green's function.

The simulation has been carried out by placing the external potentials  $V_c(r)$  on the sites of an fcc lattice and with a number of particles ( $N = 108$ ) commensurate with the lattice. At  $T = 0$ ,  ${}^4\text{He}$  crystallizes in the hcp lattice but the differences with the fcc geometry are known to be very small and would not modify the conclusions of the present work. The interatomic potential  $V(r)$  is the accurate HFD-B(HE) Aziz model<sup>21</sup> and the trial wave function used for importance sampling is a Jastrow factor  $\psi = \exp[\sum_{i<j}^N u(r_{ij})]$ , with a McMillan correlation  $u(r) = -0.5(b/r)^5$ . The parameter  $b = 1.3\sigma$  ( $\sigma = 2.556\text{\AA}$ ) is the same for all the simulations and the attractive potentials on the sites (2) are varied on its strength and range among the values  $V_0 = (500 - 800)\text{K}$  and  $\alpha = (1 - 2)\sigma^{-2}$ . These very sharp potentials are required to confine the atoms around the sites at a quantitative level comparable with the one of solid  ${}^4\text{He}$ . It is worth noticing that the localization arises due only to the branching term in the DMC algorithm since we have chosen not to include confining terms in the trial wave function to ensure a fully symmetric wave function. In order to reduce any residual bias in the calculation a preliminary study on the time-step and on the number of walkers has been carried out. In the range of confinement simulated, the energies are well behaved and their statistical errors are smaller than 1%.

## III. RESULTS

The influence of confinement on the system has been studied at a density  $\rho = 0.491\sigma^{-3}$ , which corresponds to an experimental pressure of  $\sim 34$  bar, close to the melting point of solid  ${}^4\text{He}$ . In Fig. 1, we show a projection on the  $x - y$  plane of imaginary-time trajectories of some walkers and for a given evolution time for both the present model and a DMC simulation using the NJ trial wave function (DMC-NJ) at the same localization degree. As one can see, the displacements of the atoms around the lattice sites are in both cases rather large according to the quantum nature of  ${}^4\text{He}$ . The difference between both simulations relies on the exchanges between atoms at neighboring sites, that are observed in the confining model, and which are forbidden by construction in the NJ description. With this configuration of the confining potentials the probability of hopping, i.e., the quotient between the number of MC steps where a hop is produced and the total number of steps along a simulation, is  $\sim 3\%$ .

In order to characterize the degree of localization as a function of the range and strength of  $V_c(r)$  we have calculated the density profile  $\mu(r)$  of  ${}^4\text{He}$  atoms around the lattice sites  $\{\mathbf{R}_j\}$ . From them, one can estimate the mean squared displacement

$$\langle u^2 \rangle = 4\pi \int_0^\infty \mu(r) r^4 dr, \quad (3)$$

and then the Lindemann's ratio  $\gamma = \sqrt{\langle u^2 \rangle}/a$ ,  $a$  being the nearest-neighbor distance in the lattice. In Fig. 2, results for  $\mu(r)$  for three confining models are plotted in comparison with the DMC-NJ result of solid  ${}^4\text{He}$ . The values for  $\gamma$  of the three cases are 0.192(1), 0.264(2), and 0.294(3), to be compared with the DMC-NJ value  $\gamma = 0.257$  which agrees with the experimental value  $\gamma^{\text{expt}} = 0.26$ .<sup>22</sup> All the lines in Fig. 2 are fits to the DMC results using a sum of two Gaussians, a simple model which has proved to reproduce accurately the computed data. The figure shows that the present model is flexible enough to simulate from a strongly confined system, with  $\gamma = 0.192(1)$ , until a more delocalized one, with  $\gamma = 0.294(3)$ , crossing the value of the Lindemann's ratio of solid  ${}^4\text{He}$ . As one can see, the curve of the model for  $\gamma = 0.264(2)$  is nearly indistinguishable from the DMC-NJ result.

The main objective of the present work is the estimation of the superfluid density as a function of the degree of localization of particles around the lattice sites. The superfluid density of a bosonic system may be computed with DMC by extending the winding-number technique, originally developed for PIMC calculations, to zero temperature.<sup>23</sup> Essentially, this is obtained by calculating the diffusion constant of the center of mass of the particles in the simulation box for an infinite imaginary time

$$\frac{\rho_s}{\rho} = \lim_{\tau \rightarrow \infty} \frac{1}{6N\tau} \left( \frac{D_s(\tau)}{D_0} \right), \quad (4)$$

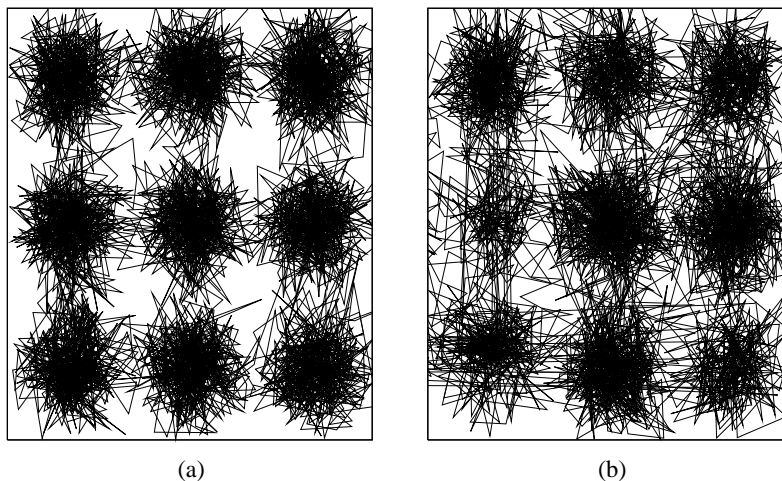


FIG. 1:  $x - y$  Projection of imaginary-time trajectories along a DMC simulation: (a) with a N-J trial wave function; (b) with the present model at the same localization ( $\gamma$ ) than case (a).

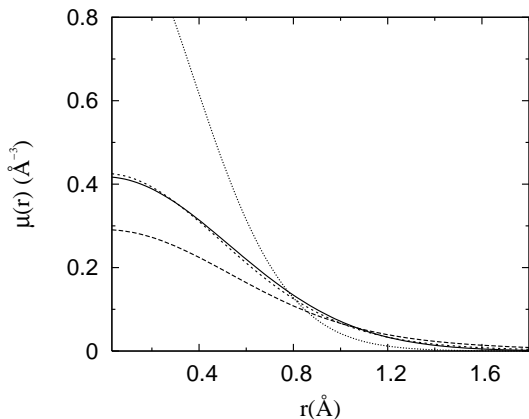


FIG. 2: Density profile,  $\mu(r)$ , of the  $^4\text{He}$  atoms around the site positions  $\{\mathbf{R}_j\}$ . The solid line corresponds to the DMC-NJ model for solid  $^4\text{He}$  ( $\gamma = 0.257$ ). Dotted, dashed, and long-dashed lines stand for the present model using potentials  $V_c(r)$  that yield  $\gamma = 0.192(1)$ ,  $0.264(2)$  and  $0.294(3)$ , respectively.

where  $D_s(\tau) = \langle (\mathbf{R}_{\text{CM}}(\tau) - \mathbf{R}_{\text{CM}}(0))^2 \rangle$ , and  $D_0 = \hbar^2/2m$ . Results obtained for  $\rho_s$  corresponding to several configurations of the lattice potentials  $V_c$  are plotted in Fig. 3. In this figure,  $\rho_s/\rho$  is shown as a function of the Lindemann's ratio of the same configuration and for values  $0.18 < \gamma < 0.30$ . The results for  $\rho_s(\gamma)$  are well parameterized by the function

$$\rho_s/\rho(\gamma) = \left[ 1 + \exp\left(-\frac{\gamma - \gamma_0}{\omega}\right) \right]^{-1}, \quad (5)$$

shown as a line in Fig. 3. The parameters in Eq. (5) are  $\gamma_0 = 0.313(4)$  and  $\omega = 0.021(1)$ . From Eq. (5) one can estimate the prediction of our model for the range of more interesting values for  $\gamma$ . In particular, considering  $\gamma^{\text{expt}} = 0.26$ , the superfluid fraction is  $\rho_s/\rho = 0.079(16)$ . It is worth noticing that the present results for  $\rho_s/\rho(\gamma)$  are qualitatively similar to the ones obtained by Saslow<sup>24</sup>

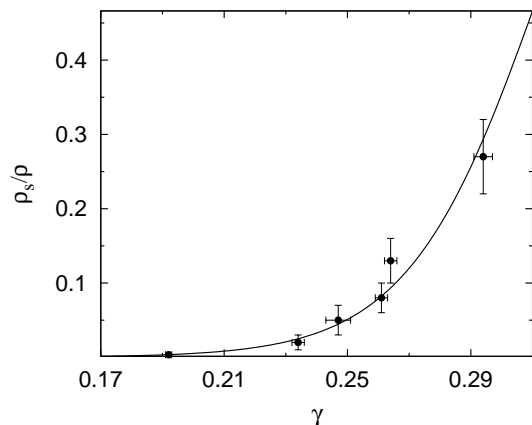


FIG. 3: The superfluid fraction as a function of the Lindemann's ratio  $\gamma$  in the localized model. The line is a fit (5) to the computed data.

assuming an uncorrelated model where all particles develop a common phase function. However, his most recent calculations predict smaller values for the superfluid fraction than ours, and in particular, for solid  $^4\text{He}$  a value  $\rho_s/\rho = 0.022$ .

The connection between the localized model here presented and the NJ description of solid  $^4\text{He}$  has been made so far by comparing the Lindemann's ratio of both calculations. To make this comparison more complete, we have explored if there are other structure properties which can also be comparable for similar values of  $\gamma$ . To this end, we have computed the two-body radial distribution function  $g(r)$ , which is proportional to the probability of finding two particles a distance  $r$  apart, and its Fourier transform, the static structure factor  $S(k)$ .

In Fig. 4, results of  $g(r)$  for two different configurations of the confining potentials  $V_c(r)$  are shown in comparison with the DMC-NJ result at the same density. These functions, as also the density profiles  $\mu(r)$  shown

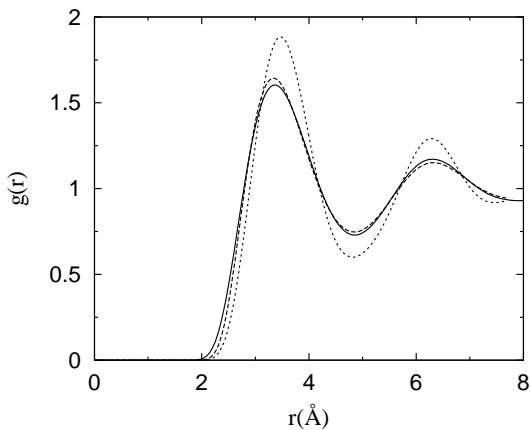


FIG. 4: Two-body radial distribution function of the localized model corresponding to superfluid fractions  $\rho_s/\rho = 0.08$  (long-dashed line) and  $0.035$  (short-dashed line). The solid line stands for the DMC-NJ result at the same density.

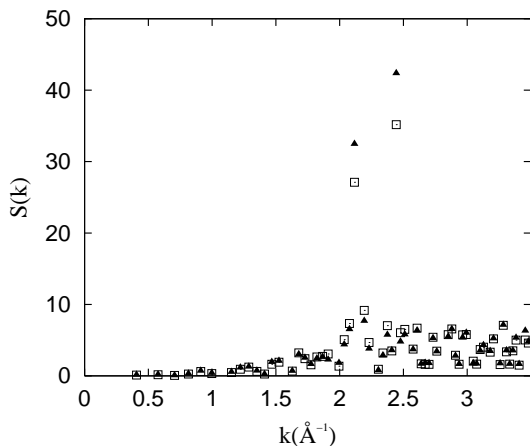


FIG. 5: Static structure factor of the localized model corresponding to  $\rho_s/\rho = 0.11$  and  $\gamma = 0.264$  (squares). The DMC-NJ result is also shown for comparison (triangles).

in Fig. 2, have been calculated using a pure estimation technique to avoid the residual bias coming from the trial wave function that the direct simulation output (mixed estimation) presents. As one can observe in the figure, when the Lindemann's ratio of the confining model is very close to the one of the NJ model both curves coincide. In the same figure, a result corresponding to a smaller  $\gamma$  value shows clearly a more pronounced peak reflecting its higher localization around the lattice sites.

The solid-like character of a given configuration is much more clear by looking at the static structure function  $S(k) = 1/N \langle \rho_{-\mathbf{k}} \rho_{\mathbf{k}} \rangle$ , with  $\rho_{\mathbf{k}} = \sum_{i=1}^N e^{i\mathbf{k} \cdot \mathbf{r}_i}$ , than  $g(r)$ . In Fig. 5, results of  $S(k)$  for the present model are compared with the DMC-NJ result for solid  ${}^4\text{He}$ . The localized model result shown in the figure corresponds to a Lindemann's ratio  $\gamma = 0.264(2)$ , close to the DMC-

NJ value for  $\gamma$ , and a superfluid fraction  $\rho_s/\rho = 0.11(1)$ . Both results show the presence of the two main first peaks at the same  $k$  values, characteristic of the underlying fcc lattice. The strength of the peaks of the localized model is slightly lower than the one of the DMC-NJ calculation since the values for  $\gamma$  in both models are not exactly the same, but it is clear that the present model is able to reproduce the expected trend of a solid phase in  $S(k)$ .

A slight trend of increasing  $\rho_s/\rho$  with pressure is evidenced on Kim and Chan's experiments,<sup>1</sup> contrarily to what it occurs in superfluid  ${}^4\text{He}$ ; the authors conjecture that this may be due to the presence of grain boundaries formed in the growth of the crystal and which affect the coherence in the superflow. Regarding this issue, we have computed  $\rho_s/\rho$  at higher density,  $\rho_u = 0.529\sigma^{-3}$ , and external constraint yielding  $\gamma = 0.264(2)$  and  $\rho_s/\rho = 0.13(3)$  at density  $\rho = 0.491\sigma^{-3}$ . The pressure of bulk solid  ${}^4\text{He}$  at density  $\rho_u$  ( $\sim 64$  bars) is still on the range of supersolid experiments. We find  $\rho_s/\rho = 0.10(2)$  and  $\gamma = 0.239(5)$  ( $\gamma = 0.246(3)$  for the DMC-NJ simulation at  $\rho_u$ ). Therefore, within the statistical uncertainties of the model we do not observe pressure dependence of  $\rho_s/\rho$  in the range of pressures analyzed.

#### IV. CONCLUSIONS

We have studied the competing effects of localization and superfluidity of bulk  ${}^4\text{He}$  immersed in a lattice of external confining potentials. The simulations have been carried out at zero temperature using the DMC method. From the curve  $\rho_s/\rho(\gamma)$ , and using the experimental value of  $\gamma$  of solid  ${}^4\text{He}$  we obtain an estimation of the superfluid fraction  $\rho_s/\rho = 0.079(16)$ , a value significantly larger than the experimental measure ( $\rho_s^{\text{expt}}/\rho = 0.01 - 0.02$ ). On top of the possible drawbacks of the localized model for describing the  ${}^4\text{He}$  solid phase, there are two effects that could help to explain the difference between the experimental measure and the present prediction. They are, first, the temperature (the simulation is at zero temperature), and second, the possible influence of impurities in the experiments. The latter can be specially relevant since, as commented by Kim and Chan,<sup>1,2</sup> a crucial point to observe superfluidity is the as much as possible elimination of impurities in the sample. The influence on the superfluid signal of  ${}^3\text{He}$  impurities and/or incommensurability can be also analyzed in the present framework. Work is in progress along this direction.

#### Acknowledgments

We acknowledge partial financial support from DGI (Spain) Grant No. FIS2005-04181 and Generalitat de Catalunya Grant No. 2005SGR-00779.

- 
- <sup>1</sup> E. Kim and M. H. W. Chan, *Nature* **427**, 225 (2004).  
<sup>2</sup> E. Kim and M. H. W. Chan, *Science* **305**, 1941 (2004).  
<sup>3</sup> E. Kim and M. H. W. Chan, *J. Low Temp. Phys.* **138**, 859 (2005).  
<sup>4</sup> A. C. Clark and M. H. W. Chan, *J. Low Temp. Phys.* **138**, 853 (2005).  
<sup>5</sup> J. Day, T. Herman, and J. Beamish, *Phys. Rev. Lett.* **95**, 035301 (2005).  
<sup>6</sup> A. F. Andreev and I. M. Lifshitz, *Sov. Phys. JETP* **29**, 1107 (1969).  
<sup>7</sup> G. V. Chester, *Phys. Rev. A* **2**, 256 (1970).  
<sup>8</sup> N. Prokof'ev and B. Svistunov, *Phys. Rev. Lett.* **94**, 155302 (2005).  
<sup>9</sup> P. W. Anderson, W. F. Brinkman, and D. A. Huse, *Science* **310**, 1164 (2005).  
<sup>10</sup> M. Boninsegni, N. Prokof'ev, and B. Svistunov, *Phys. Rev. Lett.* **96**, 105301 (2006).  
<sup>11</sup> M. W. Meisel, *Physica B* **178**, 121 (1990).  
<sup>12</sup> T. Leggett, *Science* **305**, 1921 (2004).  
<sup>13</sup> D. M. Ceperley and B. Bernu, *Phys. Rev. Lett.* **93**, 155303 (2004).  
<sup>14</sup> B. K. Clark and D. M. Ceperley, *Phys. Rev. Lett.* **96**, 105302 (2006).  
<sup>15</sup> L. Vranješ, J. Boronat, J. Casulleras, and C. Cazorla, *Phys. Rev. Lett.* **95**, 145302 (2005).  
<sup>16</sup> M. H. Kalos, M. A. Lee, P. A. Whitlock, and G. V. Chester, *Phys. Rev. B* **24**, 115 (1981).  
<sup>17</sup> L. H. Nosanow, *Phys. Rev. Lett.* **13**, 270 (1964).  
<sup>18</sup> D. Ceperley, G. V. Chester, and M. H. Kalos, *Phys. Rev. B* **17**, 1070 (1978).  
<sup>19</sup> D. E. Galli, M. Rossi, and L. Reatto, *Phys. Rev. B* **71**, 140506 (2005).  
<sup>20</sup> J. Boronat and J. Casulleras, *Phys. Rev. B* **49**, 8920 (1994).  
<sup>21</sup> R. A. Aziz, F. R. W. McCourt, and C. C. K. Wong, *Mol. Phys.* **61**, 1487 (1987).  
<sup>22</sup> C. A. Burns and E. D. Isaacs, *Phys. Rev. B* **55**, 5767 (1997).  
<sup>23</sup> S. Zhang, N. Kawashima, J. Carlson, and J. E. Gubernatis, *Phys. Rev. Lett.* **74**, 1500 (1995).  
<sup>24</sup> W. M. Saslow, *Phys. Rev. Lett.* **36**, 1151 (1976); *Phys. Rev. B* **71**, 092502 (2005).